Synthesis of graphene-coated carbon nanotubes-supported metal nanoparticles as multifunctional hybrid materials

Jaime Gallego [a], [*], Juan Tapia [a], Merlyn Vargas [a], Alexander Santamaria [a], Jahir Orozco [b], Diana Lopez [a]

[a] Química de Recursos Energéticos y Medio Ambiente, Instituto de Química, Universidad de Antioquia UdeA, Calle 70 No. 52-21, Medellín, Colombia
[b] Max Planck Tandem Group in Nanobioengineering, Universidad de Antioquia, Complejo Ruta N, Calle 67, N° 52-20, Medellín, 050010, Colombia

ARTICLE INFO

ABSTRACT

This paper presents a methodology to produce hybrid multifunctional materials based on graphene coated-metal nanoparticles supported on carbon nanotubes (M-CNT). These hybrid materials were synthetized by impregnation-reduction-decoration (IRD) methodology. Supported metal nitrates, were decomposed and reduced in-situ with CNT. After the reducing procedure, metal particles were treated with methane pulses at temperatures between 700 °C and 900 °C to encapsulate them into a few graphene sheets. These hybrid materials were characterized through different analytical techniques. In-situ X-ray diffraction analysis showed that the decomposition of nitrates occurs simultaneously with an in-situ reduction of metal particles by utilizing CNT as reducing agent. The nucleation of these metal particles preferentially starts over carbon nanotubes defects. Synthetized metal nanoparticles are active for methane decomposition, allowing the deposition of carbonaceous materials and their crystallization as graphene layers covering the metal particles (between one and four graphene layers). Magnetic characterization suggests that these hybrid materials can be used for development of magnetic storage devices, while their multifunctional properties could be potentially exploited for development of a variety of catalysts and sensors.

© 2016 Elsevier Ltd. All rights reserved.

1. Introduction

Metal-carbon nanotube (M-CNT) interfaces have been exploited in a wide range of technological developments such as metal reinforcement with CNT, electronic devices with M-CNT linkage, metals supported over CNT as catalysts and electro-magnetic devices. A wide range of metals and different types of carbon nanotubes or carbonaceous materials have been used in the above mentioned applications [1,2]. M-CNT hybrid materials have shown a good performance as magnetic materials for technological applications such as memories, magnetic drug delivery systems and (bio)sensors, among others [2–12]. The synergistic effect of hybrid materials has shown to offer improved capabilities respect to those from the concomitant individual components [4–6,13]. The fact of being composed of multiple components opens up the opportunity for developing multipurpose platforms. For example, the hybrid platform proposed herein comprises metal nanoparticles supported over CNT and decorated with some graphene layers. Such nanoengineered arrangement has not only semiconducting and magnetic properties but also potential for further functionalization. The use of inorganic particles containing hybrids, for example into biological systems, is limited by changes of their oxidation state due to variations of the biological fluid conditions such as pH and temperature [14]. This issue can be overcome by using encapsulated metal particles as core-shell systems. Encapsulating metal particles into carbonaceous materials has demonstrated to be one attractive option to obtain chemical inert materials with stable physicochemical properties. Particularly, chemical stability and reduced cytotoxicity of graphene sheets are worthy of being harnessed as metal nanoparticle-protective coat for biomedical applications.

The interactions between metals and CNT are not well characterized and understood. The nature of those interactions and their effects on the electrical and geometrical structure around M-CNT interfaces depend of the metal type as reported in literature [15,16]. Pz-orbitals of carbonaceous material surfaces interact with d-

orbitals of metals; the strength of this interaction increases with the number of unfilled d-orbitals of the metal particles. Those facts allow to predict how the supported metal solution wets the CNT surface, either decorating all its surface or generating isolated islands [15]. It is also possible to know which metal solution will have more solubility among the carbonaceous structures or which carbide has more thermodynamic favorability [17,18].

For CNT growth by catalytic chemical vapor deposition (CCVD) transition metals such as Ni, Co and Fe have been extensively used [19–21]. Commercially, Ni is the most used metal for this purpose due to its viability, low cost and good catalytic activity [22]. All three metals (as B-cation) can form a perovskite-like oxide with lanthanum as A-cation into the perovskite structure [19–21]. These perovskites, $LaMO_3$ (M: Ni, Fe, Co) have shown to be good catalyst precursors for CNT production through CCVD processes using different carbon precursors. In previous works it has been shown that $LaNiO_3$ is a proper catalyst for CNT production at temperatures between 500 °C and 900 °C using methane or ethanol as carbonaceous source [20,23]. Also other carbon sources [18,24] and catalyst precursors, such as $LaCoO_3$ and $LaFeO_3$ perovskites, have been used for CNT synthesis [25,26] obtaining different performances. Carbonaceous deposits yield, reaction temperature and carbonaceous material type depend upon the metal introduced in the perovskite structure. For example, both Ni and Co produce mainly CNT in the range of temperature from 600 °C to 800 °C, and carbon nanofibers at lower temperatures. Due to iron low reducibility, carbonaceous nanomaterials such as nanofibers can be obtained after 900 °C [19]. In a previous work, it was found that during ethanol decomposition reaction at 900 °C and using $LaFeO_3$ as catalyst precursor mainly twisted nanofibers were produced. Moreover, the presence of ethanol also helps to reduce the iron. Liu et al. used temperatures as high as 1010 °C in a mixture of CH_4 and H_2 in order to get carbon nanotubes using the same $LaFeO_3$ perovskite as catalyst precursor [26].

This paper shows a simple methodology to synthesize and characterize metal nanoparticles covered with a few graphene layers and supported over CNT (M-CNT hybrid materials). CNT were produced by ethanol decomposition reaction [19,20] using $LaMO_3$ (M: Ni, Fe and Co) perovskites as catalyst precursors. Afterwards, the same metals were supported over the CNT and encapsulated with some graphene sheets following the IRD simple methodology. The as-prepared hybrid materials not only are desirable for transformers and inductor cores, but offer great promise in the fields of catalysis and the development of sensors.

2. Experimental

2.1. Synthesis of graphene-coated CNT-supported metallic nanoparticles (M-CNT)

2.1.1. Catalysts preparation

Perovskite-like oxides were used as catalyst precursors for CNT synthesis reactions. These perovskites were obtained by self-combustion methodology as reported in previous works [19,20]. Metal (Fe, Ni or Co) nitrates salts, in an adequate molar ratio, and glycine with a molar ratio of NO^-_3/glycine = 1, were dissolved in a small amount of water. This solution was heated at 90 °C under magnetic stirring to evaporate the solvent until obtaining a gel. At this point, the temperature was quickly increased to get the glycine ignition (≈ 270 °C). The self-combustion reactions took around 10 s. Time and exothermicity depend on the metals. The powder obtained by this procedure was calcined at 700 °C in a furnace under static air atmosphere during 8 h, in order to eliminate the carbonaceous residual materials. Calcined perovskites were sieved to a particle size between 100 μm and 150 μm. Desired perovskites

(ABO_3) were based on lanthanum (A), iron, nickel and cobalt (B): $La(Ni, Fe, Co, NiFe, FeCo, NiCo)O_3$.

2.1.2. Carbon nanotubes synthesis

Carbon nanotubes were obtained through the ethanol decomposition reaction [19,20] at a reaction temperature between 700 °C and 900 °C, depending of the catalyst. The catalyst was placed on a quartz capsule into a horizontal reactor. Furnace temperature was raised at 10 °C min^{-1} under N_2 atmosphere until the desired reaction temperature (700 °C–900 °C) for 4 h. Liquid ethanol was injected at 0.04 mL min^{-1} into an evaporator system preheated at 120 °C, mixed with N_2 (22 mL min^{-1}) and conducted into the reactor. All the staling steel lines were preheated to avoid ethanol condensation.

2.1.3. Carbon nanotubes purification

The as-prepared CNT were purified by an acid treatment to dissolve the catalyst. CNT were treated with 65%-HNO_3, under continuous stirring at room temperature, for 1 h. The product was filtered and washed with deionized water until neutral pH. The residue was then dried at 100 °C for 24 h, and the CNT weight determined [20].

2.1.4. Metal impregnation

1 g of synthetized carbon nanotubes was dispersed into 50 mL of a metal (Fe, Ni or Co) nitrate solution with a concentration of 0.1% (w/v) to obtain a nominal mass fraction of 5% of M, over CNT. The dispersion was softly heated under constant magnetic stirring until complete water evaporation. After the impregnation, the materials were dried during 24 h in a conventional oven at 120 °C.

2.1.5. Encapsulation of metal particles within graphene layers

100 mg of each metal impregnated CNT were placed into a vertical quartz reactor. The temperature of the reactor was raised to 10 °C min^{-1} under argon atmosphere at 100 mL min^{-1} until 700 °C or 900 °C, in order to decompose the nitrates and reduce the metal. When the reaction temperature was reached, 100 μL pulses of pure methane were injected into the reactor using a six-way automatic valve with a frequency of 5 min (keeping the Ar flow). Gaseous products were analyzed by on-line mass spectrometry (MS) using a Pfeiffer QMS OmniStar 300c equipment.

2.2. Characterization of different M@CNT hybrid materials

2.2.1. X-ray diffraction

Diffraction patterns were recorded in an interval (2θ) from 4° to 70° with a scanning step size of 0.013° and 59 s per step. For in-situ experiments the sample was placed in a ceramic sample holder and heated under N_2 atmosphere at 10 °C min^{-1} from ambient to 700 °C, after which the reaction was hold for 1 h. XRD experiments were conducted in a Panalytical X'PERT PRO MPD diffractometer with $CuK_{\alpha 1} = 1,5406$ Å, operated at 45 kV and 40 mA.

2.2.2. Raman spectroscopy

Raman spectra were obtained in a spectral width between 10 cm^{-1} and 4000 cm^{-1} with a step of 1.5 cm^{-1} and an acquisition time of 20 s, using an Ar$^+$ laser operating at 514.5 nm. Raman spectra were deconvoluted into Lorentzian functions. The first order spectra (between 900 cm^{-1} and 2000 cm^{-1}) were fitted with four peaks (D'' $\approx$ 1166 cm^{-1}, D $\approx$ 1338 cm^{-1}, G $\approx$ 1589 cm^{-1}, D' $\approx$ 1621 cm^{-1}) and also the second order (between 2300 cm^{-1} and 3500 cm^{-1}) spectra with four peaks ((T + D) $\approx$ 2474 cm^{-1}, 2D $\approx$ 2659 cm^{-1}, (G + D) $\approx$ 2917 cm^{-1}, 2D' $\approx$ 3226 cm^{-1}).

In order to obtain statistically meaningful data, around five spectra were recorded for each sample. Raman spectra were

obtained using a HORIVA Jabin Yvon Raman U-1000 equipment with a microscopy BX 40.

2.2.3. Thermogravimetric analysis

TGA experiments were carried out in a TA-Instruments Q500 thermogravimetry analyser equipment. The analysis system was purged in N_2 for 15 min. Air flow was introduced to the system at 100 mL min^{-1} and heated at 10 °C min^{-1} until 800 °C, in order to get information about the oxidation resistance of the samples and their mineral content. To characterize the process of nitrates decomposition and in-situ reduction by effect of C_{CNT} several analyses were carried out in a N_2 atmosphere until 700 °C and holding by 1 h.

2.2.4. High resolution electron microscopy

High resolution transmission electron microscopy (HR-TEM) was carried out using a JEOL 2110 UHR instrument with a LaB$_6$ filament, at 200 kV accelerating voltage and using a JEOL ARM 200 equipped with a circular aberration correction system at 120 kV accelerating voltage. The sample was dispersed in ethanol and stirred in an ultrasound bath for 5 min. A drop of this dispersion was deposited on a Cu grid for TEM observations. Particle size and crystallographic planes were measured from HRTEM images using the public domain ImageJ [27] software platform.

2.2.5. Magnetic measurements

Magnetic measurements were carried out in a SQUID magnetometer (MPMS-XL, Quantum Design). Sample in powder form was encapsulated in Teflon tape that afterwards, was fixed inside a gelatin capsule. Magnetization curves were taken at 10 K with a maximum applied field of 7 T.

3. Results and discussion

The hybrid material presented herein comprises three well-defined processes. Synthesis of CNT with perovskite-like oxides as catalyst precursors, metal impregnation, and further encapsulation into a few graphene sheets by thermal treatment with methane pulses. Ethanol decomposition reactions were carried out with different catalyst precursors and temperatures as follow: 700 °C for Ni and Co; and 900 °C for Fe. Table 1 summarizes the CNT yields obtained at different conditions. No significant differences in the carbonaceous material yields using different catalyst precursors were observed, which is an indication that these perovskite catalyst precursors produce similar active sites for the growing of the carbon nanomaterials at the evaluated conditions.

Fig. 1 shows the thermograms obtained for the different samples, $Ni(NO_3)_2$/CNT, $Co(NO_3)_2$/CNT and $Fe(NO_3)_3$/CNT. All the supported metal nitrates are decomposed before 700 °C following three general thermal events. Nickel nitrate is decomposed at the lowest temperature while iron nitrate at the highest temperature. Metal nitrates are decomposed to their oxides passing through different intermediates as it has been reported [28–30]. The
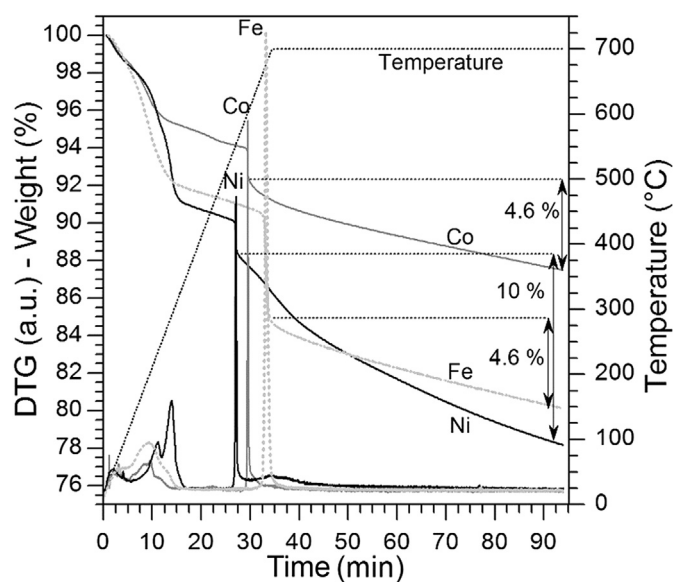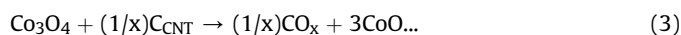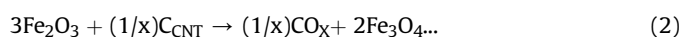
Table 1
Carbonaceous material yields (CNT as main product) after ethanol decomposition reactions using different perovskites as catalyst precursors.

Perovskite	Yield to carbonaceous materials			Reaction temperature °C
	^{a}mg	^{a}g g$_{Cat}^{-1}$	g g$_{Cat}^{-1}$ h^{-1}	
LaNiO$_3$	700	14.0	3.5	700
LaFeO$_3$	760	15.2	3.8	900
LaCoO$_3$	630	12.6	3.15	700

^{a} Obtained yield during 4 h of reaction.

Fig. 1. Thermograms in N_2 atmosphere for CNT impregnated with metal (Ni, Fe and Co) nitrates.

continuous weight lost observed after the last thermal event has been attributed to an in-situ reduction of metal oxide particles due to reaction with carbon from CNT [13], as it is schematized in Equation (1). After 1 h at 700 °C isothermal treatment in N_2, NiO$_X$/CNT sample has lost around 10% of weight while both, CoO$_X$ and FeO$_X$, only around 4.6%. It is expected that after this treatment the metals are reduced or partially reduced. The weight difference between the Ni-sample respect to Fe and Co samples shows that Ni oxides are more reactive to reduction reaction, with C as a reductive reagent, at 700 °C.

$$MO_X + C_{CNT} \rightarrow CO_X + M^0 \ldots \qquad (1)$$

Fig. 2 shows the results from in-situ XRD in N_2 atmosphere for $M(NO_3)_x$/CNT samples ($Co(NO_3)_2$; $Fe(NO_3)_3$ and $Ni(NO_3)_2$). Any diffraction pattern from nitrates was observed for the Fe sample at ambient temperature. This fact might be explained either by a good dispersion of the particles, or the presence of amorphous nitrates particles or both. For Co and Ni samples, it was possible to see the appearance of some signals corresponding to Co_2O_3 and NiO, showing that during the precipitation process of nitrates some metal oxides may be formed. As the temperature reaches 900 °C the NiO and Ni signals also increase, thus indicating higher crystallinity. Signals from the sample holder (Al_2O_3) and CNT are also evidenced during all experiments of in-situ XRD.

For the Fe sample, in situ XRD patterns show the presence of crystalline Fe_3O_4 after 300 °C. Wieczorek-Ciurowa et al. [29] reported that the thermal decomposition of pure $Fe(NO_3)_3 \cdot 9H_2O$ produces Fe_2O_3 (Fe III) at around 200 °C. For the impregnated iron nitrate over CNT, a partially reduced iron phase (Fe_3O_4 − 1Fe II and 2Fe III) was obtained. This partially thermochemical reduction was due to the effect of carbon from nanotubes over the Fe_2O_3, according to Equation (2). This partial reduction was also observed for Co sample, 1Co II and 2Co III to 3Co II (Equation (3)):

$$3Fe_2O_3 + (1/x)C_{CNT} \rightarrow (1/x)CO_X + 2Fe_3O_4 \ldots \qquad (2)$$

$$Co_3O_4 + (1/x)C_{CNT} \rightarrow (1/x)CO_X + 3CoO \ldots \qquad (3)$$
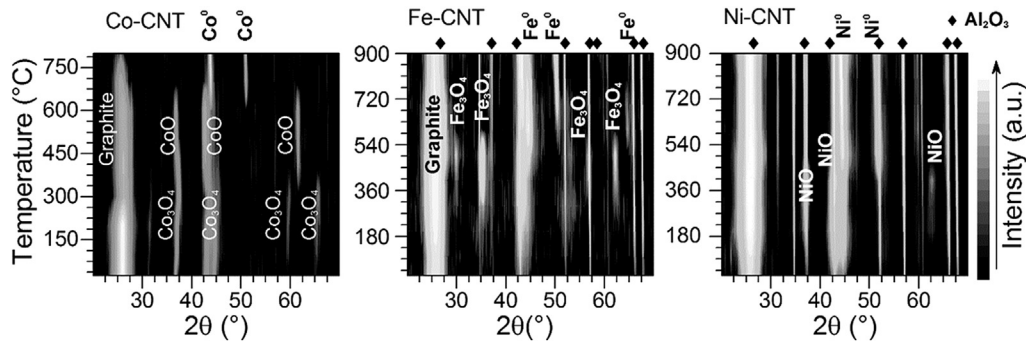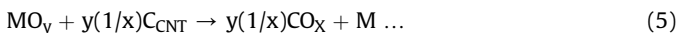
where CO_X could be either CO or CO_2.

Fig. 2. Thermal transformation of CNT-supported metal nitrates. Contour maps of in-situ XRD in N_2 atmosphere for $M(NO_3)_x$/CNT samples ($Co(NO_3)_2$; $Fe(NO_3)_3$ and $Ni(NO_3)_2$).

After 900 °C only metallic cobalt, iron or nickel crystalline phases were observed. This corroborates the high reactivity of carbon in CNT as reducing agent.

Fig. 3 shows the on-line mass profiles for the $M(NO_3)_x$/CNT samples ($Co(NO_3)_2$; $Fe(NO_3)_3$ and $Ni(NO_3)_2$). NO, NO_2, CO and CO_2 were formed during the decomposition of supported nitrates, in contrast with the reported mechanism for bulk decomposition of metal nitrates, where only NO_2 and H_2O were produced [28]. However, in this study two general thermal events with gasses evolution were observed. The first one observed around 200 °C with NO, NO_2 and CO_2 production, and the second one around 420 °C with production of CO_2, NO_2 and CO. In the first event, the production of NO may be explained by the reaction between NO_2, coming from nitrates decomposition, and C from the carbon nanotubes surface (Equation (4)).

$$2NO_2 + C_{CNT} \rightarrow 2NO + CO_2 \dots \qquad (4)$$

During the second thermal decomposition event, CO was observed and CO_2 and NO_2 signals increased in intensity. For this second decomposition, CO_2 and CO could come from the reaction between formed metal oxides after the nitrates decomposition and the carbon from CNT (Equation (5)).

$$MO_y + y(1/x)C_{CNT} \rightarrow y(1/x)CO_X + M \dots \qquad (5)$$

Where CO_X could be either CO or CO_2.

These metallic species proposed in Equation (5) can be correlated within the results achieved by the different analytical techniques used (in-situ XRD, TGA and MS0), where full decomposition of metal nitrates to obtain metallic particles and oxides supported over CNT was reached at temperatures above 700 °C.

Total consumption of methane and the highest H_2 production were obtained in the first pulse. This reaction can be explained as the decomposition of CH_4 over metal particles for producing hydrogen gas and carbonaceous deposits (Equation (6)).

$$CH_4 \rightarrow 2H_2 + C \dots \qquad (6)$$

After some methane pulses, the decomposition reaction decreased possibly due to saturation of metal particles with carbonaceous deposits.

Raman spectra for Fe, Ni and Co samples after nitrates impregnation, in-situ reduction and pulses of methane, respectively are presented in Fig. 4. This analysis does not show significant differences of graphitization (D/G ratio); and degree and surface smoothness (SO/G ratio: second order Raman scattered signals over G signal [31]) during the different treatment processes. This fact suggests that these treatments and modifications are locally affecting the carbon nanotubes but not their general structure.

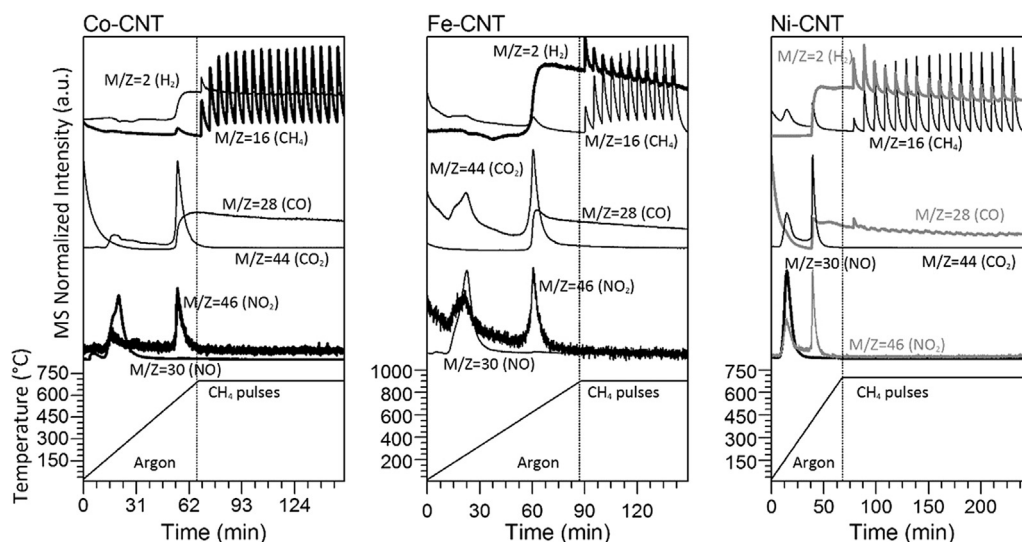General TEM micrographs are presented in Fig. 5 for raw CNT

Fig. 3. MS profiles for $M(NO_3)_x$/CNT samples ($Co(NO_3)_2$; $Fe(NO_3)_3$ and $Ni(NO_3)_2$). Thermal programmed in-situ decomposition of CNT-supported metal nitrates in Ar atmosphere and decomposition of CH_4 pulses during an isothermal step.
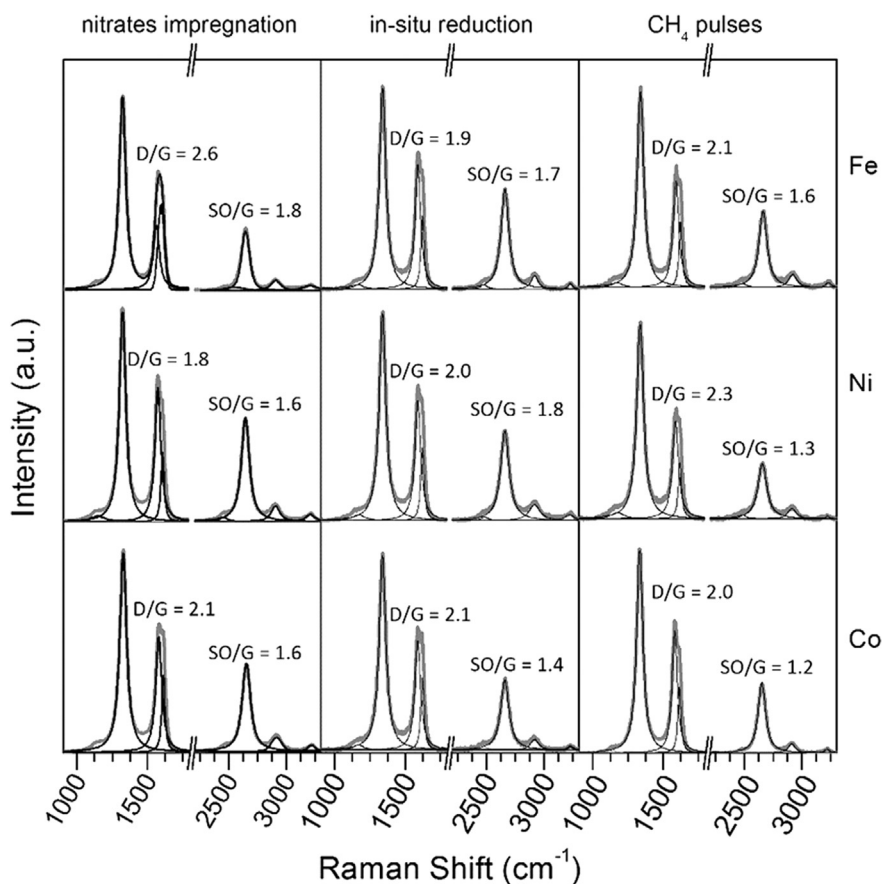
Fig. 4. Raman spectra for M-hybrid materials obtained by impregnation-reduction-decoration methodology. Spectra obtained after nitrates impregnation, thermal treatment under N_2 atmosphere (in-situ reduction) and methane pulses decomposition reaction, respectively.

obtained during ethanol decomposition reaction at 900 °C using $LaFeO_3$ as catalyst precursor (Fig. 5a), and after impregnation, in-situ reduction (b) and methane pulses decomposition (c), respectively. In a previous work, we reported the formation of twisted CNT and nanofibers using ethanol as carbon source and $LaFeO_3$ as catalyst precursor at 900 °C [19] and CNT when the catalyst precursor was $LaNiO_3$ [20]. The formation of CNT has been also reported using $LaCoO_3$ as catalyst precursor [25]. After in-situ reduction of $M(NO_3)_X$ and methane pulses decomposition, a good dispersion of metal decorated particles over CNT was observed. For the Fe@CNT sample, the histogram (see Fig. 5d) shows an average particle size of 19 nm with a standard deviation of 9 nm.

Fig. 6 shows some HR-TEM micrographs for Fe sample after methane pulses decomposition (see also Figs. 7 and 8, for Co and Ni samples, respectively). The nucleation of metal particles occurs preferentially around the structural defects of the CNT such as bamboo-like defects (Fig. 6a), the end points of a nanofiber (Fig. 7), the inner graphene closed cavities of a nanofiber (Fig. 8), and the corners formed by interaction of two CNT (Fig. 6b and c), etc. The decomposition of methane over CNT-supported metal particles produces metal particles decorated with some graphene layers, typically between two to four sheets. Gray scale profile graph, following the direction of the black arrow over Fig. 6c (inset), depicts two regions. In the first region, four gray maximums with an average separation of 0.362 nm are observed, corresponding to the separation of graphene layers with either a big curvature, or many structural defects or both. The second region shows an average separation of 0.228 nm between maximums of gray scale. These maximums might represent the <131> crystallographic plane of

tetragonal iron ($d_{131} = 0.227834$ nm, ICSD reference code 98-016-5727). For this catalytic chemical vapor deposition methodology, it is possible to obtain graphene-like structures over metal particles unlike others used approaches where metal particles are decorated with amorphous carbon deposits. Xue et al. [3] have used a pyrolytic method with a mixture of sucrose and hydrazine as carbon source to obtain a metal core-shell with amorphous carbonaceous deposits. Wang et al. [4] have reported the production of encapsulated Fe nanoparticles into different carbonaceous nanostructures such as carbon nanotubes, nanofibers, nano-onions and amorphous bulk carbonaceous deposits. These authors have used a pyrolytic method with ethanol as carbon source sprayed into a quartz reactor between 500 °C and 900 °C and iron pentacarbonyl as metal precursor. Some others procedures have been reported to obtain metal particles encapsulated into carbonaceous materials (M@C) such as levitational gas condensation [5,6], pyrolysis into an induction thermal plasma [7], plasma into a liquid system [8], among others. One of the main objectives of all the reported research is to obtain M@C hybrid magnetics materials with large coercivity, ultra-soft magnetic properties, and other special properties. The most valuable characteristic of M-C hybrid materials is that metal particles are chemically isolated, which prevents chemical changes of the inorganic species (magnetic side of the hybrid material) by reactions with external agents, such as air, acids, or other chemical or biological reagents. Unlike the previous reports, in our work we are reporting a mild methodology using aqueous impregnation and moderated temperatures. This is advantageous compared with methods such as electron beam evaporation (among other physical processes), because the
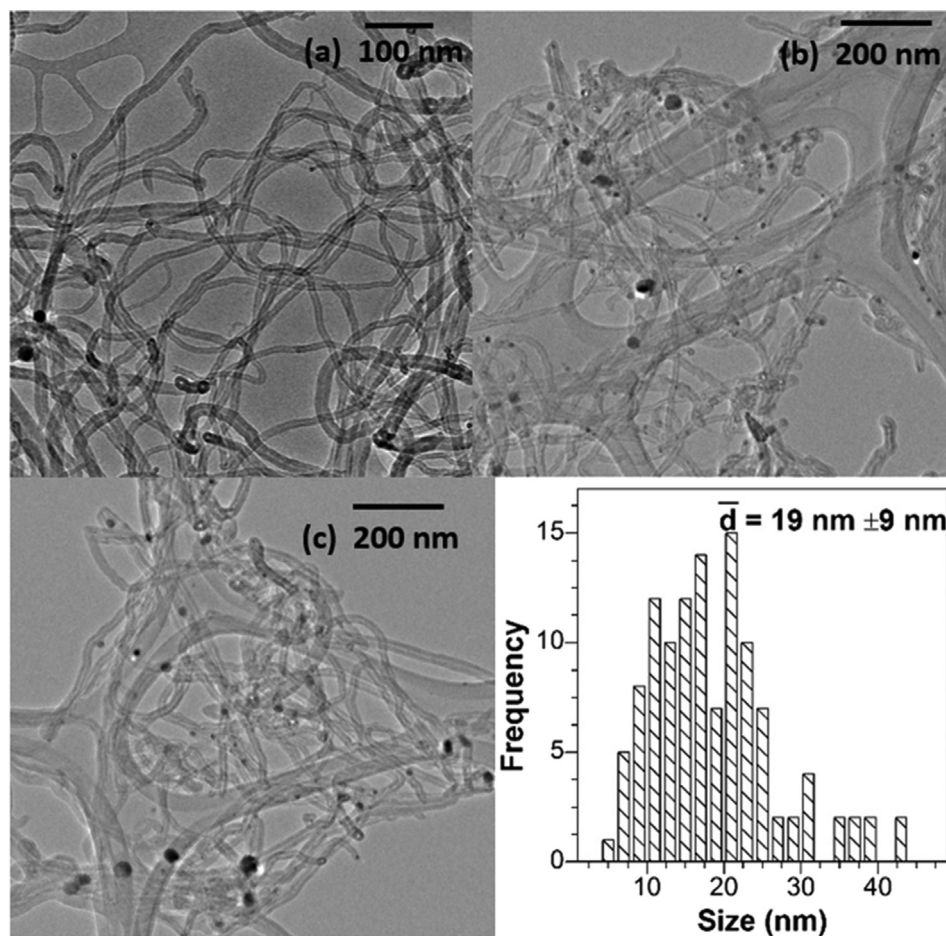
Fig. 5. TEM micrographs. Raw carbon nanotubes obtained during ethanol decomposition at 900 °C using $LaFeO_3$ as catalyst precursor (a). CNT after impregnation of $Fe(NO_3)_3$ and in-situ decomposition (b); and after methane pulses decomposition at 900 °C (c). Iron metal particle size histogram (d).
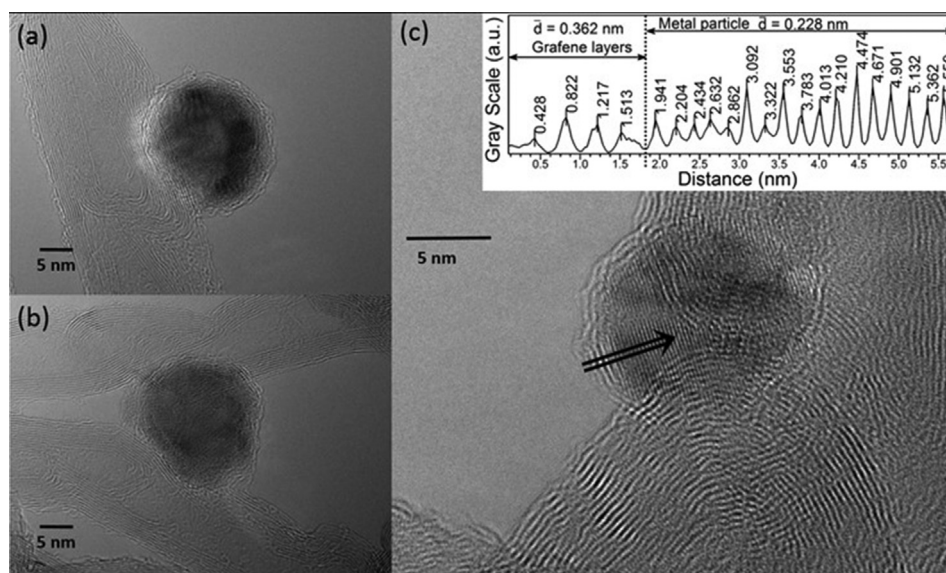

Fig. 6. HR-TEM micrographs for Fe-hybrid material (graphene-coated CNT-supported iron nanoparticles), obtained by impregnation-reduction-decoration methodology at 900 °C as final temperature.

experimental set up is cheaper; easier of tuning up and controlling the different characteristics of the desired materials. Fig. 9 shows a

schematic representation of the simple methodology reported in this paper to obtain metal-carbon based hybrid materials.
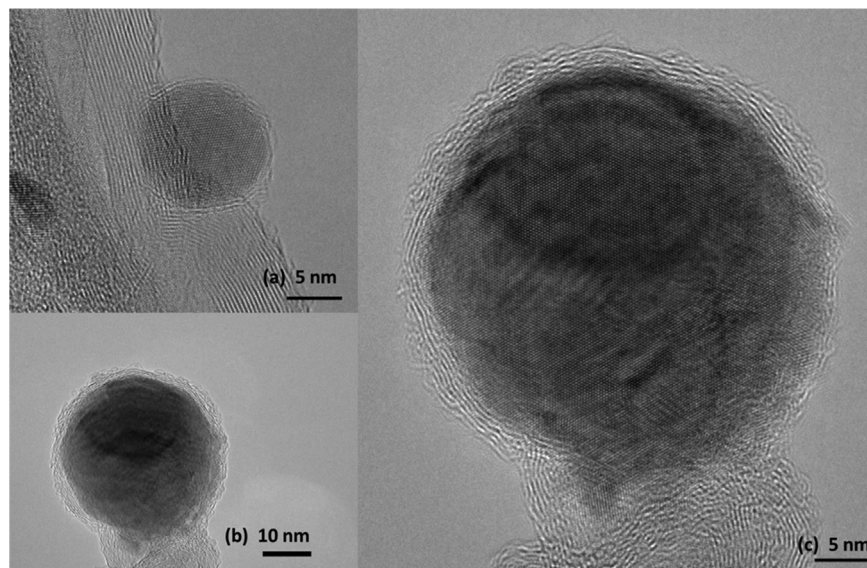
Fig. 7. HR-TEM micrographs for Co-hybrid material (graphene-coated CNT-supported cobalt nanoparticles) obtained by impregnation-reduction-decoration methodology at 700 °C as final temperature.
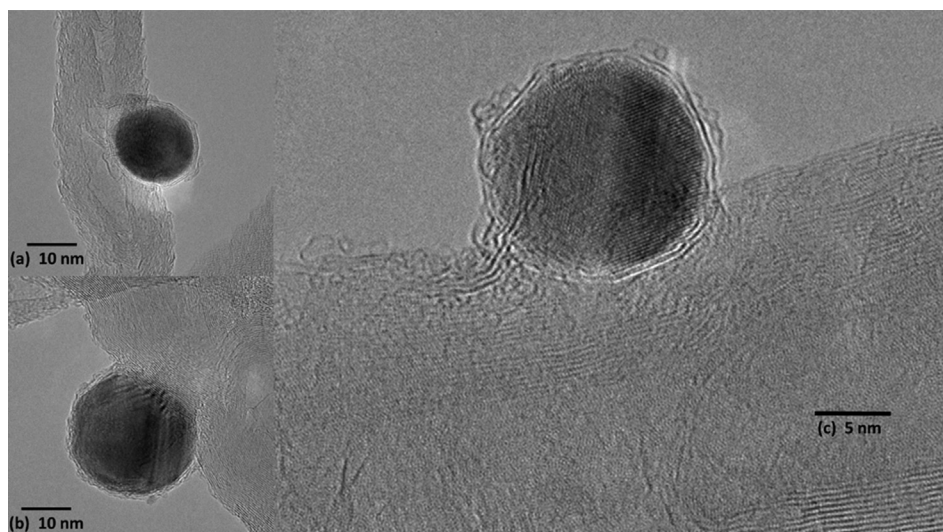

Fig. 8. HR-TEM micrographs for Ni-hybrid material (graphene-coated CNT-supported nickel nanoparticles) obtained by impregnation-reduction-decoration methodology at 700 °C as final temperature.

Some researchers have reported that Fischer-Tropsch (F-T) catalysts, iron and cobalt, present a better catalytic performance when the metal nanoparticles are placed into the inner CNT channels. This particles position avoids the deactivation processes of the F-T active phase, such as sintering and poisoning by oxidation or surface passivation. These authors attribute that to electronic and steric effects, diminishing metal particles mobility and increasing the interaction with the reaction products, with the corresponding increase of, C_{5+} hydrocarbons selectivity [32—34]. It is expected that our M-hybrid materials, at least Co- and Fe-based materials, are active with a good performance for Fischer-Tropsch synthesis.

Magnetization curves of carbon encapsulated Fe, Ni and Co nanoparticles on CNT are shown in Fig. 10. The shape of the graphs indicates a ferromagnetic response in the three samples evaluated, and the curves are symmetric around Hc = 0. The values of the squareness and coercivity (Table 2) indicate the presence of a ferromagnetic phase in each material. The results are in agreement with some previous studies where nanoparticles of Fe, Ni and Co have shown good magnetic properties when they are imbibed in a carbon based matrix [10,13,35].

Based on the resultant magnetic properties of the metal-CNT hybrid materials reported in Table 2, they are desirable for capacitors, electric engine cores, and transformers, to be applied in alternating current devices. Carbon-coated iron nanoparticles supported on CNT showed the best ferromagnetic characteristics, highest differential susceptibility and coercivity with a still high squareness. Overall, these hybrid materials hold great potential for multiple applications, including developing of sensors devices.

4. Conclusions

A simple methodology was developed to synthesize M-CNT
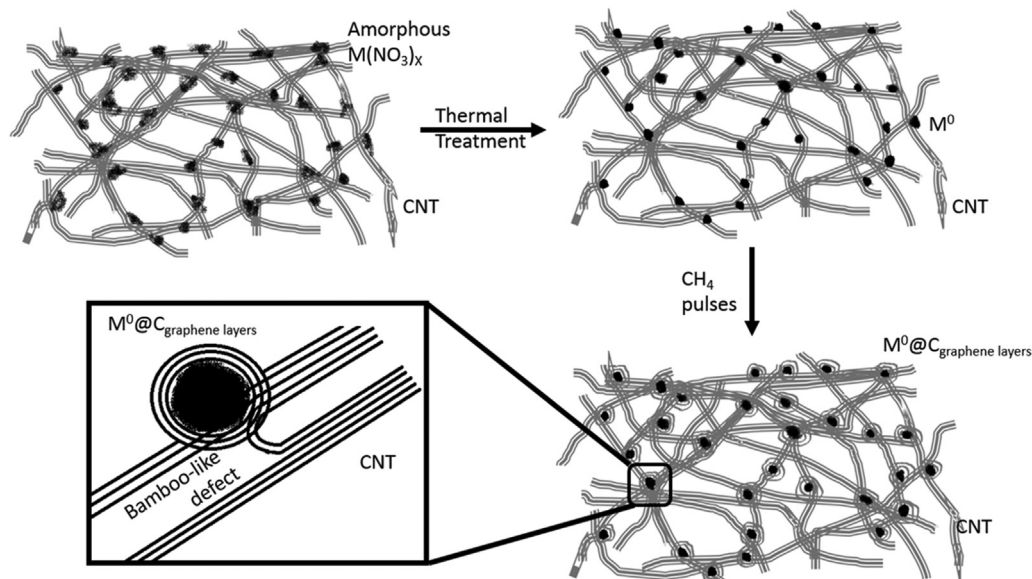
Fig. 9. Schematic representation of impregnation-reduction-decoration methodology to obtain metal-carbon hybrid materials (graphene-coated CNT-supported metal nano-particles). Metal nitrates aqueous impregnation (a), in-situ thermal decomposition-reduction metal nitrates (b) and metallic nanoparticles decoration with some graphene layers by methane pulses decomposition (c), and corresponding zoomed in area (d).
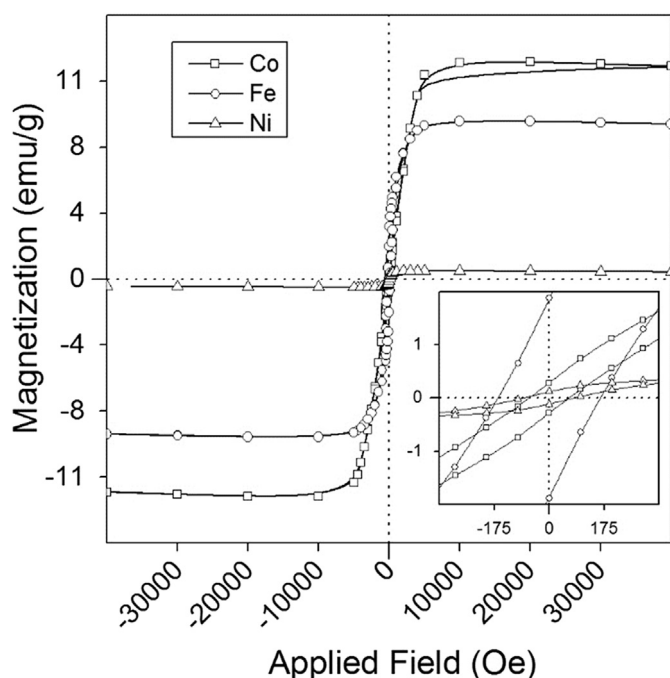

Fig. 10. Magnetization loops of M-hybrid material (graphene-coated CNT-supported Fe, Co and Ni nanoparticles) obtained by impregnation-reduction-decoration methodology.

Table 2
Different magnetic susceptibility, coercivity, remanent magnetization, saturation magnetization and squareness for M-CNT hybrid materials (graphene-coated CNT-supported nickel nanoparticles) obtained by impregnation-reduction-decoration methodology.

	Fe	Co	Ni
H_c — Coercivity (Oe)	165.4	88.2	65.4
M_r — Remanent magnetization (emu/g)	1.86	0.28	0.13
M_s — Saturation magnetization (emu/g)	8.9	12	0.46
$S = M_r/M_s$ — Squareness	0.210	0.023	0.283
H_c — of bulk material (Oe) [36]	0.05—2	10	0.7 (25—40, [37])
M_s — of bulk material at 0 K (emu/g) [38]	221.7	162.5	58.6

The main advantage of these M-CNT hybrid materials is having metal nanoparticles isolated from the atmosphere by graphene sheets, which prevent changes over metal particles and maintain their physical properties unchanged. This kind of hybrid materials is useful for catalytic reactions where a metallic phase is required. Magnetic measurements suggest that these materials are worthy of being explored in the development of alternating current and capacitor-based devices. Synergistic effect coming from the multiple components of the as-prepared hybrid materials open up a way towards the development of multipurpose platforms of enhanced properties, including sensors and catalysts.

Acknowledgements

References

[1] F. Banhart, Interactions between metals and carbon nanotubes: at the

hybrid materials. Such multifunctional materials comprise few-layer graphene-encapsulated metal particles supported on CNT. The amount of metal particles encapsulated into the hybrid material (M-CNT) was easily changed by using common reagents such as metal nitrates. In-situ reduction of metal particles by reacting with C from CNT provides a good interaction between the metallic particles and the CNT surface. This approach avoids the use of a pure carbonaceous material since the more defectiveness carbonaceous material the better distribution of the metal particles is achieved.

interface between old and new materials, Nanoscale 1 (2) (2009) 201—213.

[2] V. Georgakilas, D. Gournis, V. Tzitzios, L. Pasquato, D.M. Guldi, M. Prato, Decorating carbon nanotubes with metal or semiconductor nanoparticles, J. Mater Chem. 17 (26) (2007) 2679—2694.

[3] J. Xue, H.K. Xiang, H.Q. Ding, S.L. Pang, X.H. Wang, H. Cao, Preparation and magnetic properties of carbon encapsulated Fe-Cu alloy nanoparticles, Adv. Mater. Res. (2011) 673—676.

[4] J.N. Wang, L. Zhang, F. Yu, Z.M. Sheng, Synthesis of carbon encapsulated magnetic nanoparticles with giant coercivity by a spray pyrolysis approach, J. Phys. Chem. B 111 (8) (2007) 2119—2124.

[5] Y.R. Uhm, C.K. Rhee, Synthesis and magnetic properties of Ni and carbon coated Ni by levitational gas condensation (LGC), J. Nanomater. (2013) 2013.

[6] Y.R. Uhm, H.M. Lee, R. Chang Kyu, Structure and magnetic properties of carbon-encapsulated Ni nanoparticles, Magn. IEEE Trans. 45 (6) (2009) 2453—2455.

[7] M. Bystrzejewski, A. Huczko, H. Lange, P. Baranowski, G. Cota-Sanchez, G. Soucy, et al., Large scale continuous synthesis of carbon-encapsulated magnetic nanoparticles, Nanotechnology 18 (14) (2007).

[8] Z. Abdullaeva, E. Omurzak, C. Iwamoto, H.S. Ganapathy, S. Sulaimankulova, C. Liliang, et al., Onion-like carbon-encapsulated Co, Ni, and Fe magnetic nanoparticles with low cytotoxicity synthesized by a pulsed plasma in a liquid, Carbon 50 (5) (2012) 1776—1785.

[9] P. Singjai, K. Wongwigkarn, Y. Laosiritaworn, R. Yimnirun, S. Maensiri, Carbon encapsulated nickel nanoparticles synthesized by a modified alcohol catalytic chemical vapor deposition method, Curr. Appl. Phys. 7 (6) (2007) 662—666.

[10] D.A.S. Costa, R.V. Mambrini, L.E. Fernandez-Outon, W.A.A. Macedo, F.C.C. Moura, Magnetic adsorbent based on cobalt core nanoparticles coated with carbon filaments and nanotubes produced by chemical vapor deposition with ethanol, Chem. Eng. J. 229 (0) (2013) 35—41.

[11] E. Espinosa, R. Ionescu, B. Chambon, G. Bedis, E. Sotter, C. Bittencourt, et al., Hybrid metal oxide and multiwall carbon nanotube films for low temperature gas sensing, Sens. Actuators B Chem. 127 (1) (2007) 137—142.

[12] C.-K. Yang, J. Zhao, J. Lu, Magnetism of transition-metal/carbon-nanotube hybrid structures, Phys. Rev. Lett. 90 (25) (2003) 1—4.

[13] J. Cheng, X. Zhang, Y. Ye, Synthesis of nickel nanoparticles and carbon encapsulated nickel nanoparticles supported on carbon nanotubes, J. Solid State Chem. 179 (1) (2006) 91—95.

[14] A. Eatemadi, H. Daraee, H. Karimkhanloo, M. Kouhi, N. Zarghami, A. Akbarzadeh, et al., Carbon nanotubes: properties, synthesis, purification, and medical applications, Nanoscale Res. Lett. 9 (1) (2014) 393—406.

[15] J.J. Cha, M. Weyland, J.-F. Briere, I.P. Daykov, T.A. Arias, D.A. Muller, Three-dimensional imaging of carbon nanotubes deformed by metal Islands, Nano Lett. 7 (12) (2007) 3770—3773.

[16] Y. Zhang, N.W. Franklin, R.J. Chen, H. Dai, Metal coating on suspended carbon nanotubes and its implication to metal-tube interaction, Chem. Phys. Lett. 331 (1) (2000) 35—41.

[17] G. Wang, Y. Jin, G. Liu, Y. Li, Production of hydrogen and nanocarbon from catalytic decomposition of methane over a Ni—Fe/Al2O3 catalyst, Energy & Fuels 27 (8) (2013) 4448—4456.

[18] M. Velasquez, C. Batiot-Dupeyrat, J. Gallego, A. Santamaria, Chemical and morphological characterization of multi-walled-carbon nanotubes synthesized by carbon deposition from an ethanol—glycerol blend, Diam. Relat. Mater 50 (0) (2014) 38—48.

[19] J. Gallego, F. Mondragon, C. Batiot-Dupeyrat, Simultaneous production of hydrogen and carbon nanostructured materials from ethanol over LaNiO3 and LaFeO3 perovskites as catalyst precursors, Appl. Catal. A General 450 (0) (2013) 73—79.

[20] J. Gallego, G. Sierra, F. Mondragon, J. Barrault, C. Batiot-Dupeyrat, Synthesis of MWCNTs and hydrogen from ethanol catalytic decomposition over a Ni/La2O3 catalyst produced by the reduction of LaNiO3, Appl. Catal. A General 397 (1—2) (2011) 73—81.

[21] D. Thiele, E. Lopez-Camacho Colmenarejo, B. Grobety, A. Züttel, Synthesis of carbon nanotubes on La0.6Sr0.4CoO3 as substrate, Diam. Relat. Mater 18 (1) (2009) 34—38.

[22] R. Philippe, A. Morançais, M. Corrias, B. Caussat, Y. Kihn, P. Kalck, et al., Catalytic production of carbon nanotubes by fluidized-bed CVD, Chem. Vap. Depos. 13 (9) (2007) 447—457.

[23] G. Sierra, J. Barrault, C. Batiot-Dupeyrat, F. Mondragón, Production of hydrogen and MWCNTs by methane decomposition over catalysts originated from LaNiO3 perovskite, Catal. Today 149 (3—4) (2010) 365—371.

[24] Q. Jiang, L.J. Song, Y. Zhao, X.Y. Lu, X.T. Zhu, L. Qian, et al., Catalytic chemical vapor deposition of carbon nanotubes using Ni-La-O precursors, Mater Lett. 61 (13) (2007) 2749—2752.

[25] B.C. Liu, L.Z. Gao, Q. Liang, S.H. Tang, M.Z. Qu, Z.L. Yu, A study on carbon nanotubes prepared from catalytic decomposition of C2H2 or CH4 over the pre-reduced LaCoO3 perovskite precursor, Catal. Lett. 71 (3—4) (2001) 225—228.

[26] B.C. Liu, S.H. Tang, Z.L. Yu, B.L. Zhang, T. Chen, S.Y. Zhang, Catalytic growth of single-walled carbon nanotubes with a narrow distribution of diameters over Fe nanoparticles prepared in situ by the reduction of LaFeO3, Chem. Phys. Lett. 357 (3—4) (2002) 297—300.

[27] W. Rasband, ImageJ. 1.47c Ed. Maryland, USA, 2011.

[28] Ž.D. Živković, D.T. Živković, D.B. Grujičić, Kinetics and mechanism of the thermal decomposition of M(NO3)2·nH2O (M=Cu, Co, Ni), J. Therm. Anal. Calorim. 53 (2) (1998) 617—623.

[29] K. Wieczorek-Ciurowa, A.J. Kozak, The thermal decomposition of Fe(NO3)3·9H2O, J. Therm. Anal. Calorim. 58 (3) (1999) 647—651.

[30] W. Brockner, C. Ehrhardt, M. Gjikaj, Thermal decomposition of nickel nitrate hexahydrate, Ni(NO3)2·6H2O, in comparison to Co(NO3)2·6H2O and Ca(N-O3)2·4H2O, Thermochim. Acta 456 (1) (2007) 64—68.

[31] M.G. Donato, S. Galvagno, G. Messina, C. Milone, A. Pistone, S. Santangelo, Optimisation of gas mixture composition for the preparation of high quality MWCNT by catalytically assisted CVD, Diam. Relat. Mater 16 (4—7) (2007) 1095—1100.

[32] W. Chen, Z. Fan, X. Pan, X. Bao, Effect of confinement in carbon nanotubes on the activity of Fischer-Tropsch iron catalyst, J. Am. Chem. Soc. 130 (29) (2008) 9414—9419.

[33] A. Tavasoli, M. Trepanier, A.K. Dalai, N. Abatzoglou, Effects of Confinement in carbon nanotubes on the activity, selectivity, and lifetime of Fischer-Tropsch Co/carbon nanotube catalysts, J. Chem. Eng. Data 55 (8) (2010) 2757—2763.

[34] R.M.M. Abbaslou, A. Tavassoli, J. Soltan, A.K. Dalai, Iron catalysts supported on carbon nanotubes for Fischer—Tropsch synthesis: effect of catalytic site position, Appl. Catal. A General 367 (1—2) (2009) 47—52.

[35] V. Gupta, R.K. Kotnala, Multifunctional ferromagnetic carbon-nanotube arrays prepared by pulse-injection chemical vapor deposition, Angew. Chem. Int. Ed. 51 (12) (2012) 2916—2919.

[36] S. Tumanski, Handbook of Magnetic Measurements, CRC Press. Taylor and Francis Group, Boca Raton, 2011.

[37] M.J. Aus, B. Szpunar, A.M. El-Sherik, U. Erb, G. Palumbo, K.T. Aust, Magnetic properties of bulk nanocrystalline nickel, Scripta Metallurgica Materialia 27 (11) (1992) 1639—1643.

[38] E.P. Wohlfarth, Ferromagnetic materials, in: A Handbook on the Properties of Magnetically Ordered Substances, North-Holland Publishing Company, 1980.